Open Access
Short Paper

Journal of Agricultural Meteorology 78(4): 174–181, 2022

Interannual changes of land surface conditions in Asian dust source regions since 2000

Reiji KIMURA

(Arid Land Research Center, Tottori University, Tottori 680–0001, Japan)

Abstract

The Taklimakan and Gobi deserts and the Loess Plateau in China and Mongolia are generally recognized source areas for Asian dust. However, dust emissions depend on meteorological factors such as air pressure and land surface conditions, and precise information on land surface conditions in the dust source areas and the frequency of dust events in Japan is lacking. In this study, interannual changes of land surface conditions in the springtime since 2000 were examined in a target source region (35°N–50°N, 100°E–120°E). Back trajectory analysis results showed that most dust trajectories of the past 10 years mainly followed three routes passing over this target region. Both the number of Asian dust events observed in Japan and the area with a threshold wind speed U_t of < 10 m s^{-1} in the target region significantly decreased after 2000. Further, the area of U_t < 10 m s^{-1} and the number of events were significantly correlated. These results may reflect a decrease in the bare land surface area, which is associated with dust outbreaks.

Key words: ADE, Dust hazard, MODIS, Remote sensing

1. Introduction

Asian dust is mineral dust that is emitted from arid regions in China and Mongolia and transported toward and often deposited in remote leeward regions (Tian *et al*., 2007; Onishi *et al*., 2012; Kawai *et al*., 2021). In Japan, Asian dust degrades visibility and contaminates and soils household items, including laundry and cars. Moreover, dust events can aggravate human health problems, including asthma, allergic symptoms, and contact dermatitis (Watanabe *et al*., 2011; Otani *et al*., 2011; Higashi *et al*., 2014). For these reasons, dust monitoring and prediction are conducted in Japan by numerical simulation, remote sensing, and weather forecasting to mitigate damage caused by Asian dust (MOE, 2005).

Increased desertification (land degradation in drylands) and droughts in arid regions of northeast Asia are important factors contributing to increases in the number of Asian dust events observed in Japan (ADE) (Igarashi *et al*., 2011; Kurosaki *et al*., 2011). Thus, to improve the accuracy of numerical dust emission models it is important to clarify the effect of land surface conditions on dust occurrence (Kawai *et al*., 2021). For example, the dust outbreak frequency tends to decrease as the vegetation cover, as indicated by the normalized difference vegetation index (NDVI), increases (Kimura *et al*., 2009; Kimura and Shinoda, 2010), and dust emission modeling results are improved when vegetation is taken into account (Kang *et al*., 2014). A method for assessing land surface conditions in the dust source area is needed to obtain precise information on dust outbreaks on the Asian continent.

In this study, a method for assessing land surface conditions is proposed based on the distribution of threshold wind speeds determined by using satellite data (Kimura, 2016). Then, based on the relationship between the number of ADE in springtime and land surface conditions since 2000, a simple equation to predict the number of ADE from the area where the threshold wind speed is < 10 m s^{-1} in the dust source region is introduced.

Received; May 9, 2022
Accepted; July 21, 2022
Corresponding author: rkimura@tottori-u.ac.jp
DOI: 10.2480/agrmet.D-22-00014

2. Methods

2.1 Target region

Kimura (2012a, b) defined a target region for assessing land surface conditions for Asian dust emission as the region within 35°N–45°N and 100°E–115°E, which includes the Gobi Desert and the Loess Plateau, major dust source regions on the Asian continent (Sun *et al*., 2001; Lim and Chun, 2006; Shao and Dong, 2006). Kimura (2012a, b) showed that the increasing trend in vegetation coverage (decreasing trend in the bare surface area) from 2000 to 2011 in this target region corresponded to a decreasing trend in dust storm frequency and ADE. In addition, Tian *et al*. (2007), who examined the relationship between ADE and dust storm frequency in northern China, reported that dust storm frequency in Inner Mongolia and the number of ADE varied mostly in parallel from 1967 to 2006.

Therefore, in this study, the target region was expanded to the region within 35°N–50°N and 100°E–120°E (2,731,268 km^2), which includes northeastern Mongolia, Inner Mongolia, and northeast China as well as the Gobi Desert and the Loess Plateau (Fig. 1). This target region approximately coincides with the CN region (northeastern Asian continent) defined by the Japan Meteorological Agency (JMA) for back trajectory analyses (https://ds.data.jma.go.jp/ghg/kanshi/trajectory/info_trajectory.html) and the major dust outbreak region (40°N–50°N, 100°E–120°E) defined by the Japanese Ministry of the Environment (MOE, 2018).

To verify that the air masses transporting Asian dust passed over this target region in these past ten years (2012–2021), the NOAA HYSPLIT model (Stein *et al*., 2015; Rolph *et al*., 2017) (https://www.ready.noaa.gov/HYSPLIT_traj.php) was used to calculate back trajectories for 96 hours (4 days) from 500 m altitude over Fukuoka City (33.59°N, 130.40°E) (MOE, 2018) on dates when ADE were observed. Fukuoka was selected as the end point because on average 60% of ADE observed annually since 2000 affected Fukuoka.

2.2 Assessing land surface conditions in the target region and ADE

According to an analysis using weather data, strong wind significantly affects dust events in northeast Asia (Lim and Chun, 2006; Shao and Dong, 2006). However, the driving force of the strong wind varies among dust source regions because of differences in the land surface characteristics. Thus, consideration of surface conditions, such as vegetation and snow cover, which have an important effect on the dust events is also required. Firstly, Kimura (2012a, b) examined simply the relationship between ADE and land surface conditions as indicated by the NDVI-based vegetation cover. Later, Kimura (2016) developed a satellite-based method for mapping dust erodibility in the area within 35°N–50°N and 75°E–120°E. In this method, based on the threshold wind speed for dust emission (U_t) at 10 m height the region is categorized into severe (bare land), moderate (sparse vegetation), and nearly no dust hazard (vegetation reducing dust outbreaks, snow cover, wet surface, and frozen soil) areas (Table 1).

In this study, the areal coverage of each land surface type was mapped and annual changes in their coverages were compared to changes in the number of springtime ADE since 2000. The mapping system, which uses Moderate Resolution Imaging Spectroradiometer (MODIS) satellite data on snow cover, area of frozen soil, land surface wetness, and vegetation cover can be summarized as follows (see Kimura, 2016, for details of the calculation process): First, if snow cover and frozen soil are absent, dust events are assumed to be possible. Second, if the land surface wetness determined from the Satellite-based Aridity Index (SbAI) (Kimura and Moriyama, 2014) exceeds a threshold value (= 0.03), dust events are assumed to be possible. Finally, U_t at 10 m height is calculated from the NDVI following the method of Kimura and Shinoda (2010). Determinations of cloud and snow cover are derived from cloud and snow flag information in the satellite data. "Frozen soil" status is assumed when the satellite-determined land surface temperature is below 273.15 K.

For the calculations and analysis, MODIS data products (MOD09A1, MOD09CMG, and MOD11C1) for spring (March to May) from 2000 to 2021 were used. Daily satellite data were downloaded from the Land Processes Distributed Active Archive Center (https://earthdata.nasa.gov/eosdis/daacs/lpdaac), and the dust erodibility map was updated in semi-real time. To minimize the effect of clouds during analysis periods, which is large in 1-day data products, 16-day composite products were

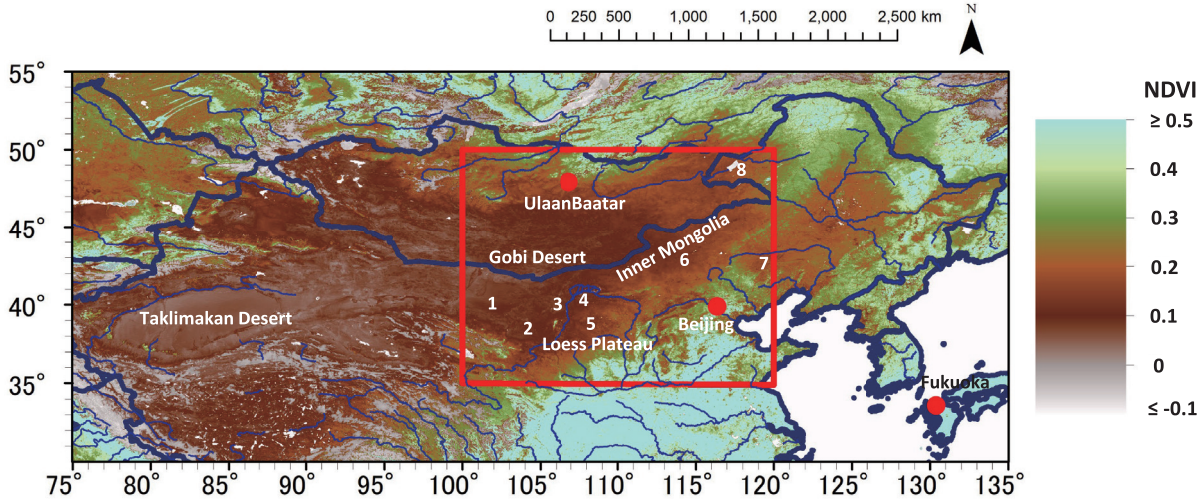

Fig. 1. Distribution of NDVI values in East Asia, based on the MODIS 1 km product in April 2020. The red rectangle indicates the target region defined in this study. The numbers indicate desert or sandy lands in the target region: 1, Badain Jaran desert; 2, Tengger desert; 3, Ulan Buh desert; 4, Hobq desert; 5, Mu Us sandy land; 6, Otindag sandy land; 7, Horqin sandy land; and 8, Hulunbeir sandy land.

Table 1. Dust hazard level based on the threshold wind speed U_t. Other categories are snow cover, frozen soil, and a wet surface. The land surface types were defined on the basis of the NDVI range (Kimura, 2012a, b).

Dust hazard level	U_t (m s^{-1})	NDVI	Land surface type
severe dust	$U_t < 10$	$0.05 \leq$ NDVI < 0.1	bare land (A)
moderate dust	$10 \leq U_t < 15$	$0.1 \leq$ NDVI < 0.2	sparse vegetation (B)
nearly no dust	$U_t \geq 15$	NDVI ≥ 0.2	vegetation reducing dust outbreaks (C)
	others	-----	snow cover (D), wet surface (E), frozen soil (F)

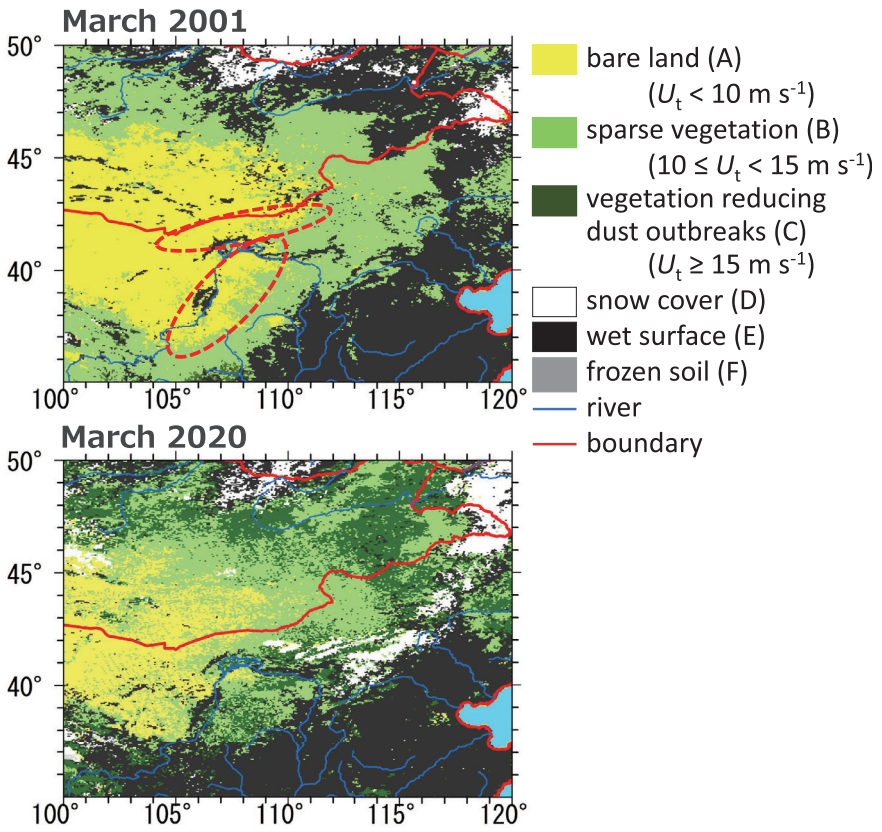

Fig. 2. Distribution map of each land surface type in the target region based on the threshold wind speed U_t in March 2001 and 2020. Red broken line ellipses on the March 2001 map show parts of Inner Mongolia and the Loess Plateau where the area with U_t < 10 m s^{-1} (bare land) is obviously larger in 2001 compared with 2020.

prepared. The reason why 16-day composite was used is that the 16-day composite SbAI was a better indicator to avoid the effect of cloud cover than 8-day composite SbAI. The final spatial resolution was 0.05°. The 16-day data in each month was finally averaged as monthly.

According to the above-described method, the assumed dust hazard level was based on U_t and corresponded to the categories A to F in the land surface type, that is, bare land (A), sparse vegetation (B), vegetation reducing dust outbreaks (C), snow cover (D), wet surface (E), and frozen soil (F) (Table 1). The approximate range of NDVI corresponding to each U_t range is also shown (Kimura and Shinoda, 2010). Fig. 2 shows the distribution map of each land surface type categorized in the Table.

Kurosaki and Mikami (2005) reported that U_t was less than 10 m s^{-1} at 50 (77%) out of 65 SYNOP meteorological observatories within the target region, and at 15 (23%) observatories, U_t was either more than 10 m s^{-1} or less than 15 m s^{-1}. When U_t is 15 m s^{-1}, dust events are effectively eliminated because instances of wind speeds exceeding 15 m s^{-1} are rare in northeast Asia (Kurosaki and Mikami, 2005).

The number of ADE from March through May during the 22 years from 2000 was obtained from the JMA (https://www.data.jma.go.jp/gmd/env/kosahp/kosa_Table_1.html). Note that this dataset contains the monthly "number of days" on which an ADE was observed at one or more of the 61 JMA observatories. Therefore, even if many observatories observed an event on a given day, only one ADE would be counted on that day.

3. Results and discussion

3.1 Interannual changes in the number of ADE from 2000

The total number of ADE from March through May significantly decreased from 2000 to 2021 (Fig. 3). From 2012 to 2020, an ADE was observed on fewer than 10 days each year,

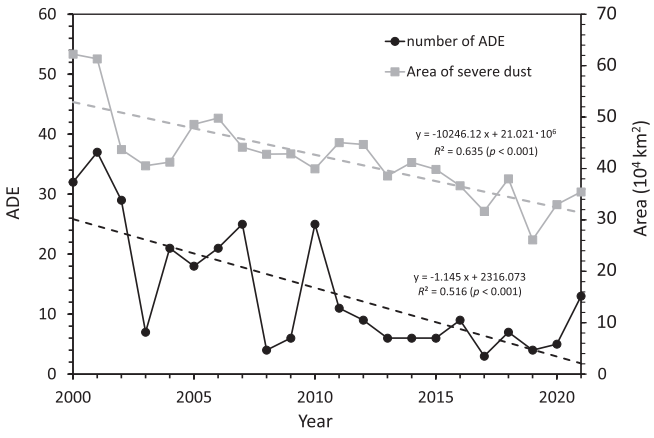

Fig. 3. Interannual changes in the number of ADE from March to May during 2000–2021 and in the U_t < 10 m s^{-1} area in the target source region.

but in 2021 ADE were observed on 13 days. Although more ADE were observed in 2021 than had been observed during the previous decade, however, the normal value (average values for the last 30 years) observed annually from 1991 to 2020 as determined by JMA was 13 days; thus, the number of ADE in 2021 did not exceed the normal value.

3.2 Transport routes of Asian dust and dust source areas

Asian dust was observed in Fukuoka on 43 days in these past ten years (2012-2021) (Fig. 4); on 40 days the trajectories passed through the defined target region, and on the other three days, they passed through the region between 120°E and 130°E (10 May 2021, 4 April 2020, and 7 April 2018). Many other back trajectory analyses of ADE have also shown that the dust source was in the defined target area (e.g., Onishi *et al*., 2012; MOE, 2014; Uno *et al*., 2017; Tsedendamba *et al*., 2019). The 40 trajectories passing through the target region can be roughly classified into three routes.

- Route (a): Eastern Mongolia (110°E–120°E) → Inner Mongolia (14 days)
- Route (b): Central Mongolia (100°E–110°E) → Gobi Desert → Inner Mongolia (22 days)
- Route (c): Western China deserts (1 to 5 in Fig. 1) → Loess Plateau (4 days)

According to MOE (2014), most Asian dust trajectories from 2003 to 2012 passed through Mongolia and the inner region of China, in agreement with the defined target region of this study.

Thus, in recent decades not only Mongolia, the Gobi Desert, and the Loess Plateau but also Inner Mongolia and northeastern China have been Asian dust source regions (Tian *et al*., 2007; Minamoto *et al*., 2018). Moreover, Tian *et al*. (2007) and Kurosaki *et al*. (2016) have reported that dust storm frequencies at SYNOP stations in Inner Mongolia and ADE varied nearly in parallel from the middle of the 1970s to the end of 1990s. In the region within 35°N–50°N and 105°E–120°E, high northerly or northwesterly wind speeds with cyclonic activity are remarkable (Tian *et al*., 2007), which favors dust outbreaks (Tian *et al*., 2007; Yamamoto and Hayakawa, 2008). Although in this study, the dust outbreak frequency in the target region was not examined, high dust outbreak frequencies were observed there during the 2000s (Kurosaki and Mikami, 2005; Wu and Kai, 2016; Kawai *et al*., 2021; Bao *et al*., 2021).

3.3 Effect of land surface conditions in the target region on ADE

Table 2 shows the correlation between the coverage of each land surface category (see Table 1) in each month, which was calculated every 16-day interval of MODIS data, and ADE from March through May using the area of 35°N–50°N and 100°E–120°E. The number of ADE from 2000 to 2021 showed a significant positive correlation with land surface category A coverage (bare land; $U_t < 10$ m s^{-1}) during the springtime and a significant negative correlation with category C coverage (vegetation reducing dust outbreaks; $U_t \geq 15$ m s^{-1}) except in May. A negative but nonsignificant correlation was found between category D coverage (snow cover) and the number of ADE. However, category H coverage (= C + D) showed a significant negative correlation with the number of ADE in April and during March–May considered together. In general, category E (wet surfaces) and F (frozen soil) surfaces are thought to inhibit dust occurrence, but a significant negative correlation was observed between category E and the number of ADE only in May.

The effects of category A and B (sparse vegetation; $10 \leq U_t < 15$ m s^{-1}) coverages observed here are similar to the findings of Kurosaki and Mikami (2005), who reported that U_t was less than 10 m s^{-1} at 77% of 65 SYNOP meteorological observatories within the target region, and between 10 and 15 m s^{-1} at the remaining 23% of the observatories.

The significant correlations between category A and C coverages and the number of ADE may reflect less bare land or more vegetation. Both the number of ADE and category A coverage have been declining since 2000 (Fig. 3). The Chinese government has initiated national projects (e.g., Grain for Green Program in 1999, and Phase 2 of the Three-North Shelter Forest Program in 2001) and invested substantial resources to combat desertification and promote greening in arid regions (Cao *et al*., 2009; Li *et al*., 2012). As a result of these efforts, vegetation has gradually increased, as shown by some satellite data (IPCC, 2019; Chen *et al*., 2019; Kimura, 2017). The spatial distribution of each land surface type in the target region during March 2001 (the year with the largest number of ADE during the study period) shows that the coverage of bare land was larger in 2001 than in 2020 (the year with small number of ADE), especially in Inner Mongolia and on the Loess Plateau (Fig. 2). Although the reduction in the number of ADE cannot be definitely attributed to these Chinese projects, at least with regard to dust sources in China, statistical analyses suggest that the greening has had some effect on dust occurrences (CAS, 2018; Long *et al*., 2018; Wu and Kai, 2016; Tan and Li, 2015).

The number of ADE was calculated using the following simple regression equation, where the explanatory variable was selected by considering multicollinearity.

$$\mathrm{ADE} = 9.23 \cdot 10^{-5} X - 25.08 \ (R = 0.74, p < 0.001), \quad (1)$$

where X is the category A coverage (km^2). Then, the relationship between the total observed and calculated numbers of ADE from March through May (Table 2) was examined (Fig. 5). The root mean square error (RMSE) was 7 days, which is within the normal number of ADE (= 13 days), but in 2002, 2008, and 2010, the estimated error was more than 10 days. Simulation results obtained with the Regional Atmospheric Modeling System and a synoptic weather analysis showed that slight changes in the air pressure distribution, the transport route of Asian dust, and the amount of dust transportation in the atmospheric boundary layer led to large differences in the number of ADE in those years (Hara *et al*., 2004; MOE, 2014). Therefore, the accuracy of ADE estimation with Eq. (1) depends on prevailing meteorological conditions. In addition, the instantaneous dust events would be suppressed by coverages of categories C, D, E, and F. However, Eq. (1), which was obtained by using 16-day composite MODIS products, can be used to determine whether the number of ADE during March–May is likely to be more or less than the normal

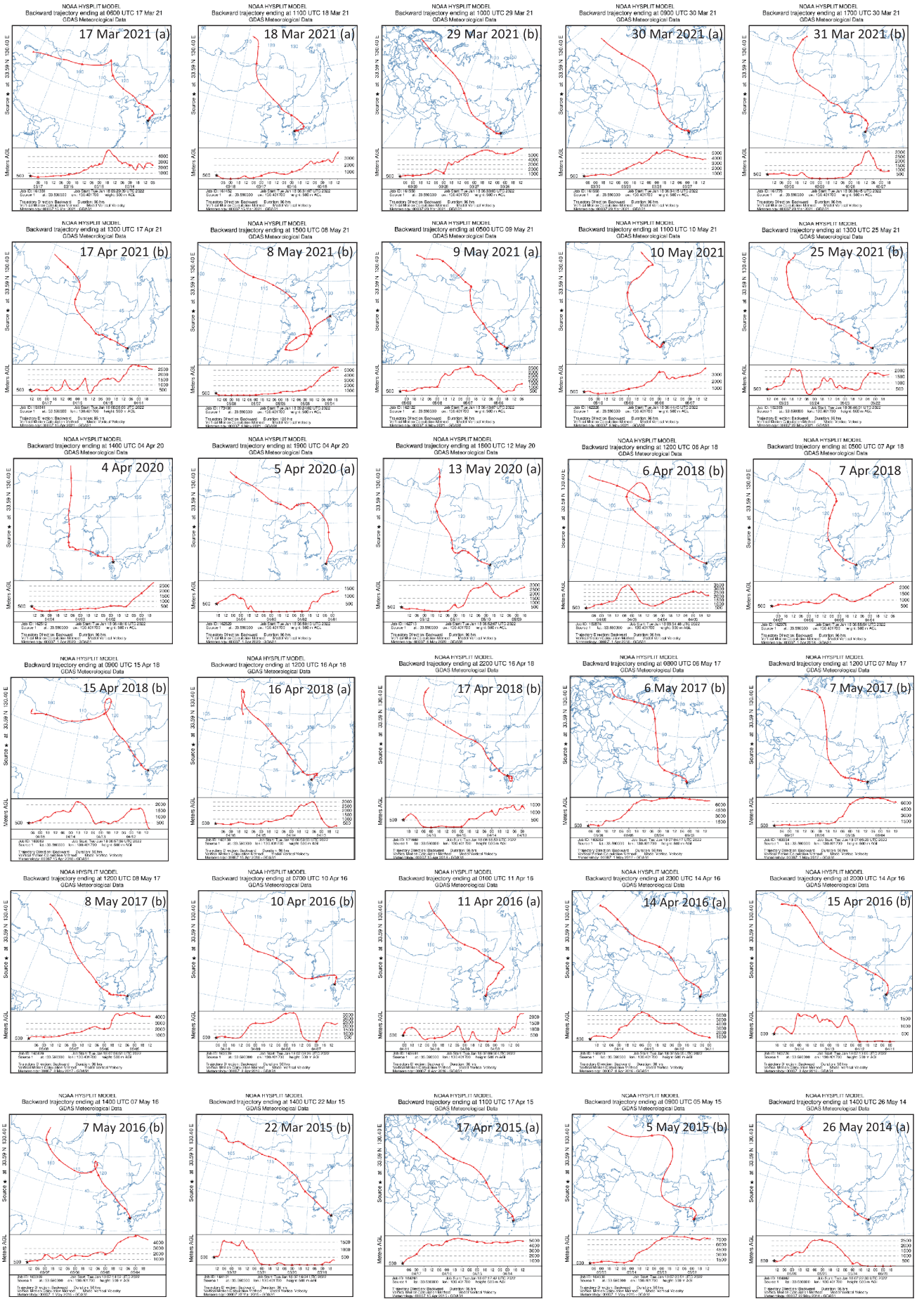

Fig. 4. (continued)

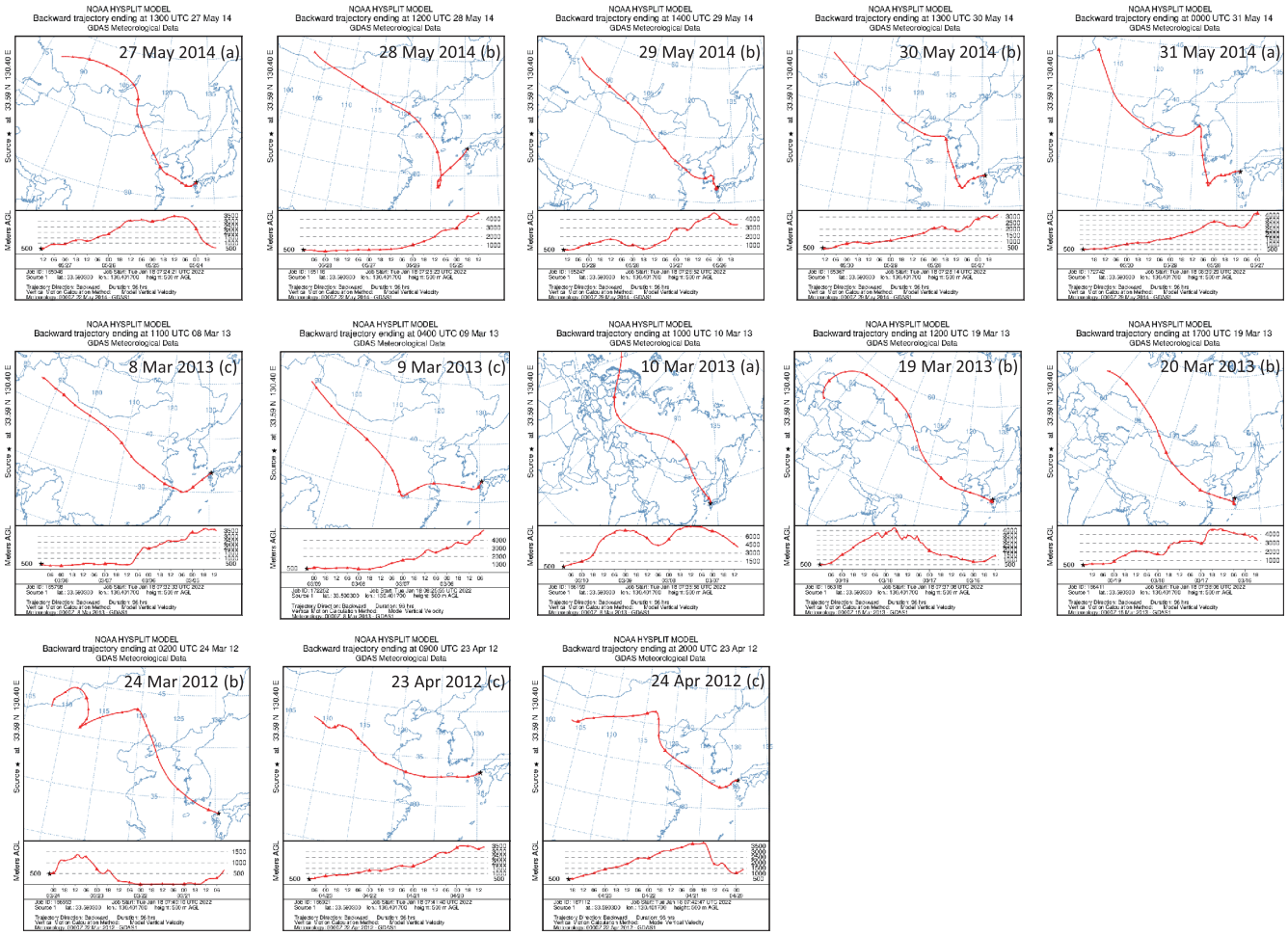

Fig. 4. Backward trajectories ending at 500 m altitude above Fukuoka City obtained by using the NOAA HYSPLIT model in these past ten years (2012–2021). (a), (b), and (c) indicates the classified routes in this study.

Table 2. Correlation coefficients (r) between the coverage of each land surface category in each month and ADE from March through May. p-values are shown in parentheses, and n.s. means not significant. Significant values are highlighted in yellow.

Land surface type	March	April	May	Total
bare land (A)	0.66 ($p < .001$)	0.63 ($p < .01$)	0.77 ($p < .001$)	0.74 ($p < .001$)
sparse vegetation (B)	0.08 (n.s.)	0.25 (n.s.)	0.54 ($p < .01$)	0.38 (n.s.)
vegetation reducing dust outbreaks (C)	−0.44 ($p < .05$)	−0.51 ($p < .05$)	−0.33 (n.s.)	−0.50 ($p < .05$)
snow cover (D)	−0.14 (n.s.)	−0.22 (n.s.)	−0.29 (n.s.)	−0.18 (n.s.)
wet surface (E)	0.10 (n.s.)	0.05 (n.s.)	−0.54 ($p < .01$)	−0.24 (n.s.)
frozen soil (F)	0.19 (n.s.)	0.23 (n.s.)	−0.33 (n.s.)	0.21 (n.s.)
(A) + (B) (G)	0.33 (n.s.)	0.41 (n.s.)	0.67 ($p < .001$)	0.57 ($p < .01$)
(C) + (D) (H)	−0.37 (n.s.)	−0.54 ($p < .01$)	−0.35 (n.s.)	−0.50 ($p < .05$)

value at the 77% probability level. The threshold category A coverage to obtain the normal number of ADE was 412,567 km^2.

Conclusions

The spatial distribution of threshold wind speed during the springtime (March to May) in northeast Asia was mapped to assess land surface conditions in dust source regions since 2000. The region within 35°N–50°N and 100°E–120°E was targeted in this study, and most dust trajectories during the past ten years passed through this target region. Trajectories passing through Mongolia, the Gobi Desert, the Loess Plateau and Inner Mongolia, were roughly grouped into three routes.

The annual number of ADE significantly decreased after 2000. Therefore, the relationship between the coverage area of various threshold wind speed (U_t) ranges and the number of ADE was analyzed. ADE showed a significant positive correlation with the coverage of $U_t < 10$ m s^{-1}, and a significant negative correlation with the coverage of $U_t \geq 15$ m s^{-1}. These significant correlations

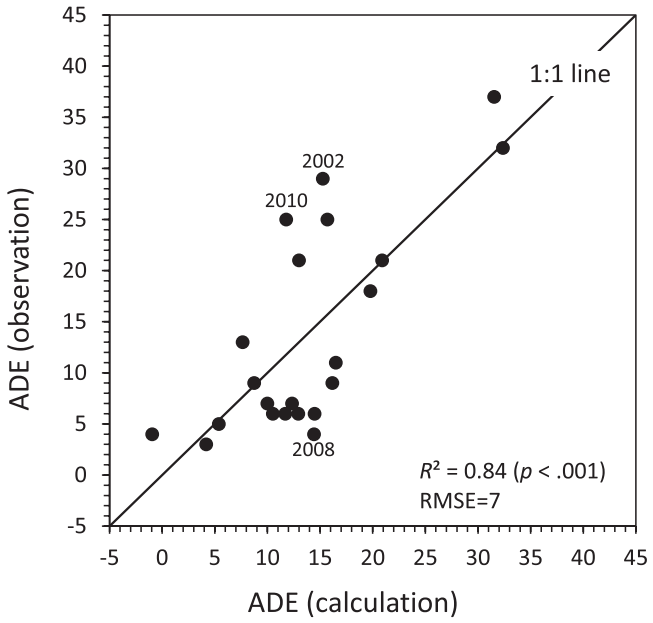

Fig. 5. Relationship between the observed and calculated number of ADE based on the coverage of U_t < 10 m s^{-1} from March through May.

may reflect enhancements or reductions of dust outbreaks due to changes in the bare land surface and vegetation coverages. The RMSE between the observed number of ADE and the number calculated using the coverage of U_t < 10 m s^{-1} from March through May was 7 days.

Accuracy of this method is limited if the dust source region includes areas outside of the target region or if the transport route is different. However, the results of this study and previous studies indicate that most ADE from March to May are affected mainly by dust events in the target region. Thus, this method, if combined with consideration of the atmospheric transport route, is potentially a useful tool for predicting whether the number of ADE in a given year will be larger or smaller than the number in a normal year. It is my hope that the usefulness of the method presented here will be confirmed generally, and that it will become useful in the near future for assessing land surface conditions in dust source areas.

Acknowledgements

This research was funded by a Grant-in-Aid for Scientific Research, grant number KAKENHI 19H04239. I appreciate the valuable comments from two reviewers and associate editor of this paper.

References

Bao T, Gao T, Nandintsetseg, B *et al*., 2021: Variations in frequency and intensity of dust events crossing the Mongolia-China border. *SOLA* **17**, 145–150.

Cao S, Chen L, Yu X, 2009: Impact of China's Grain for Green Project on the landscape of vulnerable arid and semi-arid agricultural regions: a case study in northern Shaanxi Province. *Journal of Applied Ecology* **46**, 536–543.

CAS (Chinese Academy of Sciences), 2018: Three-North Shelterbelt Program completed afforestation of 46.14 million hectares over the past 40 years. A press release by CAS, https://english.cas.cn/newsroom/archive/news_archive/nu2018/201812/t20181228_202988.shtml.

Chen C, Park T, Wang X, *et al*., 2019: China and India lead in greening of the world through land-use management. *Nature Sustainability* **2**, 122–129.

Hara Y, Satake S, Uno I *et al*., 2004: Interannual variations of 'Kosa' simulated by a regional-scale dust transport model. *Tenki* **51**, 719–728.

Higashi T, Kambayashi Y, Ohkura N *et al*., 2014: Exacerbation of daily cough and allergic symptoms in adult patients with chronic cough by Asian dust: A hospital-based study in Kanazawa. *Atmospheric Environment* **97**, 537–543.

Igarashi Y, Fujiwara H, Jugder D, 2011: Change of the Asian dust source region deduced from the relationship between anthropogenic radionuclides in surface soil and precipitation in Mongolia. *Atmospheric Chemistry and Physics* **11**, 7069–7080.

IPCC, 2019: *Climate Change and Land: an IPCC special report on climate change, desertification, land degradation, sustainable land management, food security, and greenhouse gas fluxes in terrestrial ecosystems*. In press.

Kang JY, Tanaka TY, Mikami M, 2014: Effect of dead leaves on early spring dust emission in East Asia. *Atmospheric Environment* **86**, 35–46.

Kawai K, Matsui H, Kimura R *et al*., 2021: High sensitivity of Asian dust emission, transport, and climate impacts to threshold friction velocity. *SOLA* **17**, 239–245.

Kimura R, 2012a: Factors contributing to dust storms in source regions producing the yellow-sand phenomena observed in Japan from 1993 to 2002. *Journal of Arid Environments* **80**, 40–44.

Kimura R, 2012b: Effect of the strong wind and land cover in dust source regions on the Asian dust event over Japan from 2000 to 2011. *SOLA* **8**, 77–80.

Kimura R, 2016: Satellite-based mapping of dust erodibility in northeast Asia. *Natural Hazards* **92**, 19–25.

Kimura R, 2017: Validation and application of the monitoring method for degraded land area based on a dust erodibility in eastern Asia. *International Journal of Remote Sensing* **38**, 4553–4564.

Kimura R, Moriyama M, 2014: Application of a satellite-based aridity index in dust source regions of northeast Asia. *Journal of Arid Environments* **109**, 31–38.

Kimura R, Shinoda M, 2010: Spatial distribution of threshold wind speeds for dust outbreaks in northeast Asia. *Geomorphology* **114**, 319–325.

Kimura R, Bai L, Wang J, 2009: Relationships among dust outbreaks, vegetation cover, and surface soil water content on the Loess Plateau of China, 1999–2000. *Catena* **77**, 292–296.

Kurosaki Y, Mikami M, 2005: A study on aeolian dust outbreak in east Asia. Research Report, Tsukuba, Japan, pp. 139. (in Japanese)

Kurosaki Y, Shinoda M, Mikami M, 2011: What caused a recent increase in dust outbreaks over East Asia? *Geophysical Research Letters* **38**, L11702, doi:10.1029/2011GL047494.

Kurosaki Y, Kurozawa Y, Shinoda M *et al*., 2016: *Asian dust: Effects on human health and environment, and counter measures*. Maruzen Publishing, Tokyo, Japan, pp. 150. (in Japanese)

Li M, Liu A, Zou C *et al*., 2012: An overview of the "Three-North" Shelterbelt project in China. *Forestry Studies in China* **14**, 70–79.

Lim JY, Chun Y, 2006: The characteristics of Asian dust events in Northeast Asia during the springtime from 1993 to 2004. *Global and Planetary Change* **52**, 231–247.

Long X, Tie X, Li G *et al*., 2018: Effect of ecological restoration programs on dust pollution in North China Plain: a case study. *Atmospheric Chemistry and Physics* **18**, 6353–6366.

Minamoto Y, Nakamura K, Wang M *et al*., 2018: Large-scale dust event in east Asia in May 2017: Dust emission and transport from multiple source regions. *SOLA* **14**, 33–38.

MOE, 2005: *The special committee report on dust and sandstorm issues*. Government of Japan, Tokyo, Japan, pp. 112. (in Japanese)

MOE, 2014: *Report on surveys of the reality of Kosa*. Government of Japan, Tokyo, Japan, pp. 143. (in Japanese)

MOE, 2018: *Report on surveys of the Asian dust transport in 28th year of the Heisei period*. Ministry of the Environment, Tokyo, Japan, pp. 86. (in Japanese)

Onishi K, Kurosaki Y, Otani S *et al*., 2012: Atmospheric transport route determines components of Asian dust and health effects in Japan. *Atmospheric Environment* **49**, 94–102.

Otani S, Onishi K, Mu H *et al*., 2011: The effect of Asian dust events on the daily symptoms in Yonago, Japan: A pilot study on healthy subjects. *Archives of Environmental & Occupational Health* **66**, 43–46.

Rolph G, Stein A, Stunder B, 2017: Real-time environmental applications and display system: READY. *Environmental Modelling & Software* **95**, 210–228.

Shao Y, Dong CH, 2006: A review on East Asian dust storm climate, modeling and monitoring. *Global and Planetary Change* **52**, 1–22.

Stein AF, Draxler RR, Rolph GD *et al*., 2015: NOAA's HYSPLIT atmospheric transport and dispersion modeling system. *Bulletin of the American Meteorological Society* **96**, 2059–2077.

Sun J, Zhang M, Liu T, 2001: Spatial and temporal characteristics of dust storms in China and its surrounding regions, 1960–1999: relations to source area and climate. *Journal of Geophysical Research* **106**, 10325–10333.

Tan M, Li X, 2015: Does the green great wall effectively decrease dust storm intensity in China? A study based on NOAA NDVI and weather station data. *Land Use Policy* **43**, 42–47.

Tian SF, Inoue M, Du M, 2007: Influence of dust storm frequency in northern China on fluctuations of Asian dust frequency observed in Japan. *SOLA* **3**, 121–124.

Tsedendamba P, Jugder D, Baba K *et al*., 2019: Northeast Asian dust transport: Case study of a dust storm event from 28 March to 2 April 2012. Atmosphere **10**, 69, doi:10.3390/atmos10020069.

Uno I, Yumimoto K, Pan X *et al*., 2017: Simultaneous dust and pollutant transport over east Asia: The tripartite environment ministers meeting March 2014 case study. *SOLA* **13**, 47–52.

Watanabe M, Yamasaki A, Burioka N *et al*., 2011: Correlation between Asian dust storms and worsening asthma in western Japan. *Allergology International* **60**, 267–275.

Wu J, Kai K, 2016: Characteristics of dust outbreaks and their relation to strong wind and land surface conditions in the Gobi desert and northern China, 1999–2013. *SOLA* **26**, 51–57.

Yamamoto N, Hayakawa S, 2008: The relationship between El Niño, La Niña, the number of dust-storm days near the Gobi Desert, and yellow-sand events in Kyushu, Japan. *Journal of Environmental Information Science* **22**, 115–120. (in Japanese)